Product internal-state distribution for the reaction $H + HI \rightarrow H_2 + I$

Dahv A. V. Kliner,[a] Klaus-Dieter Rinnen,[b] Mark A. Buntine, David E. Adelman, and Richard N. Zare
Department of Chemistry, Stanford University, Stanford, California 94305

(Received 21 February 1991; accepted 25 April 1991)

We have measured the nascent H_2 (v, j) product-state distribution from the $H + HI \rightarrow H_2 + I$ abstraction reaction. Laser photolysis of HI at 266 nm generated translationally hot H atoms with center-of-mass collision energies of 1.61 and 0.68 eV in the ratio 64:36. Quantum-state-specific detection of the molecular reaction product was accomplished via (2 + 1) resonance-enhanced multiphoton ionization and time-of-flight mass spectrometry. The H_2 is formed with a high degree of internal excitation, including a vibrational population inversion between $v = 0$ and $v = 1$. Our product-state distribution agrees closely with that of Aker, Germann, and Valentini where comparison is possible. Rotational population distributions derived from the quasiclassical trajectory calculations of González and Sayós are generally too cold, whereas those of Aker and Valentini nearly reproduce the experimental distributions. Both calculations fail to predict, however, the observed vibrational inversion.

I. INTRODUCTION

The atom–diatom abstraction reaction

$$H + HI \rightarrow H_2 + I \tag{1}$$

is an extreme example of the mass combination light + light –heavy → light–light + heavy. This mass combination causes the skew angle in the H + HI mass-weighted coordinate system to be $\gamma = 45°$.[1] This kinematic feature suggests that about one half ($\cos^2 \gamma$) of the incident translational energy is unavailable for internal excitation of the reaction products.

The H + HI abstraction reaction is very exothermic ($\Delta H = -1.424$ eV),[2] and therefore possesses a potential energy surface (PES) with an early barrier. In such systems, there is a propensity to convert reagent translational energy into product vibrational energy,[1,3] although this tendency is mitigated by the kinematic constraint mentioned above. The experimentally determined activation energy is 0.031 ± 0.011 eV between 230 and 297 K.[4] Such a small activation energy is expected for a system with an early barrier. Another aspect of the energetics for this reaction is the possible production of electronically excited $I^*(^2P_{1/2})$ [0.943 eV above ground state $I(^2P_{3/2})$].[5] Infrared chemiluminescence studies at thermal energies have demonstrated that $> 98.0 \pm 1.5\%$ of the I atoms are produced in the ground electronic state;[6] the I*/I branching ratio is unknown at higher collision energies, although ion-imaging measurements suggest that it is nonzero.[7]

The exchange reaction,

$$H + H'I \rightarrow HI + H', \tag{2}$$

competes with abstraction [reaction (1)]. A barrier to I-atom exchange of 0.42 eV has been calculated.[8] Kinetic studies at 300 K show that abstraction is the dominant channel for both H + DI ($96 \pm 4\%$) and D + HI ($88 \pm 8\%$).[9] Two crossed molecular beam studies of the D + HI exchange reaction at superthermal collision energies have determined total reaction cross sections. McDonald and Herschbach[10] measured a value of approximately 1–10 Å^2 at a center-of-mass collision energy (E_{rel}) of about 0.3 eV. Bauer, Rusin, and Toennies[11] obtained a value of 2.4 ± 0.7 Å^2 at $E_{rel} \approx 0.2$ eV.

Partial quantum-state resolution of the D_2 product of the D + DI reaction was achieved by Continetti, Robinson, and Lee.[12] A beam of DI was photolyzed to generate D atoms with $E_{rel} = 1.8$ or 3.2 eV, which reacted with the remaining DI in the beam. Time-of-flight distributions of the D_2 indicated that this reaction product was highly internally excited.

Full quantum-state resolution of the H_2 product of the H + HI reaction was first achieved by Aker, Germann, and Valentini (AGV).[13] Photolysis of HI at 266 nm generated H atoms with $E_{rel} = 1.61$ and 0.68 eV in the concetration ratio 0.64:0.36,[14] corresponding to the production of I and I*, respectively. These workers used coherent anti-Stokes Raman spectroscopy (CARS) to measure the internal-state distribution of the H_2 product of the H + HI reaction. Similar experiments were carried out for the H + HBr and H + HCl abstraction reactions. AGV found a propensity to conserve translational energy in this series of reactions, i.e., the translational energies of the reactants and products were approximately equal and the product internal energies corresponded to the reaction exoergicities. They noted that the energy of the highest populated rotational level in each vibrational state was nearly equal to the reaction exoergicity plus $E_{rel}/2$. The factor of 1/2 was interpreted as the projection of the incident translational energy on the product translational coordinate in the mass-weighted coordinate system ($\cos^2 \gamma = 1/2$ for $\gamma = 45°$). In a complementary study, Aker, Germann, Tabor, and Valentini[15] measured the internal-state distributions of the HX (X = halogen) exchange/inelastic products of these reactions. For both the abstraction and exchange/inelastic channels, absolute cross sections were measured. The total cross section for the

[a] Present address: Department of Chemistry, University of Minnesota, Minneapolis, MN 55455.
[b] Present address: AT&T Bell Laboratories, Room 1D354, 600 Mountain Avenue, Murray Hill, NJ 07974.

$H + HI$ abstraction reaction was determined to be 2 ± 1 Å^2,[13] while a value of 11 ± 2 Å^2 for $H + HI$ exchange/inelastic collisions was found.[15] It was argued that this latter cross section is dominated by the exchange reaction rather than by inelastic scattering.[15]

Quantum-state-specific detection of H_2 may also be achieved with $(2+1)$ resonance-enhanced multiphoton ionization (REMPI),[16] which has higher sensitivity than CARS. Previously, REMPI has been used to investigate the effect of indistinguishable nuclei on the $H + HI$ (Ref. 17) and $D + DI$ (Ref. 18) abstraction reactions. This detection method was also applied to the $H + HI$ abstraction reaction to produce the first ion images of a bimolecular reaction.[7]

In this paper we report the $H_2(v, j)$ product state distribution from the $H + HI \rightarrow H_2 + I$ reaction. We used laser photolysis of HI at 266 nm to generate translationally hot H atoms, which initiated the reaction. Quantum-state-specific detection of the molecular reaction product was accomplished via $(2+1)$ REMPI and time-of-flight mass spectrometry (TOF/MS). We have observed H_2 reaction product in 72 rotational levels spread over 4 vibrational states. The H_2 is formed with a high degree of internal excitation, including a vibrational population inversion between $v = 0$ and $v = 1$. There is excellent agreement between our population distribution and that of AGV where comparison is possible. Thus, the experimental H_2 internal-state distribution can be used to test theoretical treatments of the reaction dynamics for this simple system.

II. EXPERIMENT

The apparatus was identical to that used for our studies of the $H + H_2$ reaction family[19–21] and so is only briefly described here. HI (Matheson, 97% stated purity) was purified by a freeze–pump–thaw cycle immediately prior to use and was stored in a Teflon-lined stainless steel cylinder. The decay rate of the HI in the gas handling and storage system was measured to be less than 0.3% per hour. The HI effusively flowed from a vertical, capillary glass nozzle (3–10 Torr backing pressure) into a high-vacuum chamber (5×10^{-8} Torr base pressure). Photolysis of the HI beam by a 5 ns, 266 nm laser pulse (Spectra-Physics Nd:YAG fourth harmonic, DCR-1A or injection-seeded GCR-4, 10 Hz) generated translationally hot H atoms with center-of-mass collision energies of 1.61 and 0.68 eV in the ratio of 64:36.[14] The photolysis beam was collimated to a diameter of ~ 3 mm and passed ~ 2 mm below the nozzle. We calculate that less than 5% of the HI was photolyzed under our experimental conditions. Because of thermal motions of the reagents, the spread in the collision energy was 0.08 eV for the fast channel and 0.05 eV for the slow channel.[22] Reaction occurred with the remaining HI that had not been photolyzed, i.e., the same gas provided both reagents.

A second (probe) laser, tunable between 201 and 240 nm, was fired approximately 60 ns after the photolysis laser to ionize the H_2 reaction product via REMPI. The probe-laser beam was collinear and counterpropagating with respect to the photolysis beam and was focused by a 125 mm lens. The probe light was generated by frequency doubling and sum-frequency mixing (INRAD Autotracker II) the output of a Nd:YAG-pumped dye laser (Spectra-Physics, DCR-3G, PDL-1, 10 Hz) using β-barium borate (BBO)[23] crystals. The ions were accelerated into a shuttered TOF/MS[19] and the time-gated ion signal was recorded with a computer-interfaced CAMAC system,[24] which also controlled the scanning of the probe laser. The detection procedure has been calibrated against a high-temperature effusive nozzle, enabling the majority of the measured ion signals to be related to relative quantum state populations[16] (see Results section).

In the absence of the photolysis laser, H_2^+ ions were still detected. This resulted from probe-laser photolysis of HI, i.e., the probe laser effected both photolysis and detection of the reaction product within a single laser pulse.[25] The probe-laser-induced reaction signal was subtracted from the total signal on a shot-by-shot basis to obtain the 266 nm induced distributions. The subtraction procedure has been described in Ref. 20 (method 2). There was also a small H_2^+ signal present independent of the probe-laser wavelength. This nonresonant signal, which was typically a few percent of the total ion signal, probably originated from the charge-transfer reaction $I^+ + H_2 \rightarrow H_2^+ + I$.[26] It was of no consequence for the present study; the small baseline offset that it caused was removed by the subtraction procedure.

In the course of our previous measurements on the $H + H_2$ reaction family, studies were performed to ensure that the observed signal was from the nascent reaction product.[20,21] Because the present experiment was carried out under conditions similar to those of the previous experiments (and often with lower reagent pressure), it was expected that we were still operating within the single-collision regime. To verify this conjecture, the $H_2(v = 1, j)$ distribution from the $H + HI$ reaction was recorded as a function of delay time between the photolysis and probe laser pulses. No change in this distribution was observed for delays between 40 and 100 ns. In addition, the $H_2(v = 1, j)$ distribution from the probe-laser-induced $H + HI$ reaction was recorded as a function of nozzle backing pressure. No change was observed for pressures ranging from 4.5 to 9.0 Torr. We conclude that the observed H_2^+ signal corresponded to the nascent product of the $H + HI$ reaction.

The REMPI signal is a measure of the *density* of a given H_2 rovibrational state at the temporal and spatial position of the probe-laser focus (nominally 0.1 mm in diam), which was contained within the much larger photolysis beam (~ 3 mm in diam). The study of the $H_2(v = 1, j)$ product rotational distribution as a function of delay time between the photolysis- and probe-laser pulses demonstrated that product flyout from the detection volume was negligible for delays of less than 100 ns. That is, about the same number of product molecules entered the detection volume as exited during this time. Consequently, the detection sensitivity was independent of the velocity of the product molecules. A simple calculation indicates that this conclusion is reasonable. The fastest H_2 product molecules had a speed of $\sim 17\,000$ m/s and traveled 1.5 mm (half of the photolysis-laser spot size) in ~ 90 ns. Thus, the measured $H_2(v, j)$ density (ion signal) corresponds to the *time-integrated flux* of reaction product into that state.

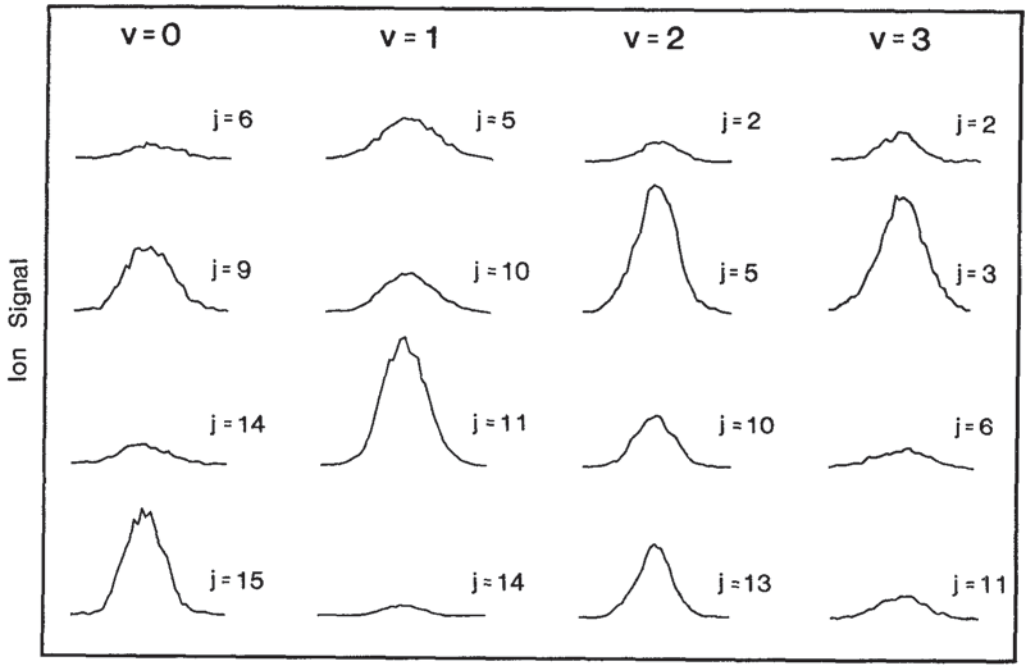

FIG. 1. Representative spectral peaks of the H_2 (v, j) product of the H + HI reaction. Each peak represents one scan, which took 150–750 s. See text for additional experimental conditions.

III. RESULTS

Figure 1 shows representative spectral peaks of the H_2 (v,j) product of the H + HI reaction. Spectra were recorded with a time constant of 2–10 s. Such spectral peaks were corrected for probe-laser pulse energy and integrated to obtain relative quantum-state populations of the nascent H_2 reaction product. Recall that the REMPI signal is a measure of the density of a given H_2 rovibrational state, corresponding to the time-integrated flux of reaction product into that state (Sec. II). The observed product rovibrational distributions are therefore a measure of relative *rates* of reaction into those states, i.e., the present measurements correspond to state-specific rate constants.

As previously mentioned, 266 nm photolysis of HI generates H atoms with H + HI center-of-mass collision energies of 1.61 and 0.68 eV in the ratio of 64:36.[14] Because both collision energies are well above the 0.03 eV barrier to the abstraction reaction,[4] the measured internal-state distribution contains contributions from two collision energies. The individual contribution of each collision energy could not be isolated with the present experimental configuration. Because we measured specific rate constants, not cross sections, the relative contribution of each channel is given by the product of the photolysis branching ratio into that channel and its relative velocity. Therefore, the measured rate constants correspond to 64% of the 1.61 eV rate constant plus 36% of the 0.68 eV rate constant, or 73% of the 1.61 eV cross section plus 27% of the 0.68 eV cross section.

For each vibrational state, the rotational distribution was recorded at least 10 times. The rotational distributions are listed in Table I and plotted in Fig. 2. As shown in Table I, there is a marked population alternation between adjacent rotational levels of the H_2 product of the H + HI reaction. These alternations are a consequence of the indistinguishability of the H nuclei in this system.[17,18] The rotational distributions shown in the figures have been corrected for nuclear indistinguishability by multiplying by 3 the populations of the even (*para*-) j levels.

The calibration of the REMPI-TOF/MS detection procedure allowed the derivation of correction factors to convert measured ion signals into relative quantum-state populations.[16] The range of calibrated rovibrational levels is smaller than that populated by the H + HI reaction. Specifically, we have calibrated the H_2 rovibrational levels ($v = 0$, $j = 0$, 2–4, 6–15), ($v = 1, j = 2$–11, 13), and ($v = 2, j = 2$–7). There are three types of entries in Table I and in the figures:

(i) *Populations*, i.e., calibrated ion signals. These are denoted by the entries in the table without parentheses (solid circles in the figures).

(ii) *Estimated populations* obtained from ion signals using estimated calibration factors. For the calibrated levels, the experimental correction factors were generally in close agreement with those derived from calculated two-photon cross sections.[27] For most of these levels, the experimentally and theoretically determined correction factors were unity; it was found that there is tunneling in the H_2 $E,F\,^1\Sigma_g^+$ state for levels that have nonunity correction factors ($j \geqslant 11$ for H_2).[16,27] Therefore, for uncalibrated $j < 11$ levels where the calculations of the two-photon cross sections predict unit correction factors, we applied factors of unity. These levels are denoted by parentheses in the table (half-filled circles in the figures).

(iii) *Uncalibrated ion signals*. Correction factors were not estimated for uncalibrated levels for which tunneling occurs in the E,F state ($j \geqslant 11$).[16,27] For these levels, we report measured ion signals, which constitute lower limits on the actual populations. Experimental calibration factors would be necessary to convert their values to populations. These entries are given in square brackets in the table (open

TABLE I. H + HI→H_2 (v,j) + I rotational population distributions.

	Relative population[a]			
j	$v=0$	$v=1$	$v=2$	$v=3$
0	···	(0.029 ± 0.003)	(0.042 ± 0.004)	(0.104 ± 0.012)
1	···	(0.187 ± 0.011)	(0.47 ± 0.04)	(0.83 ± 0.04)
2	0.06 ± 0.03	0.117 ± 0.009	0.228 ± 0.018	(0.54 ± 0.05)
3	0.34 ± 0.12	0.45 ± 0.02	0.96 ± 0.05	(2.5 ± 0.3)
4	0.108 ± 0.018	0.206 ± 0.017	0.36 ± 0.03	(0.82 ± 0.06)
5	(0.39 ± 0.08)	0.79 ± 0.04	1.29 ± 0.08	(1.81 ± 0.15)
6	0.151 ± 0.013	0.280 ± 0.013	0.51 ± 0.03	(0.35 ± 0.04)
7	0.54 ± 0.05	0.91 ± 0.05	1.58 ± 0.11	(0.94 ± 0.11)
8	0.26 ± 0.02	0.382 ± 0.015	(0.54 ± 0.03)	(0.27 ± 0.05)
9	0.79 ± 0.05	1.42 ± 0.09	(1.43 ± 0.08)	(0.78 ± 0.17)
10	0.33 ± 0.03	0.67 ± 0.04	(0.37 ± 0.02)	(0.20 ± 0.04)
11	1.01 ± 0.13	2.3 ± 0.5	[0.88 ± 0.09]	[0.51 ± 0.09]
12	0.59 ± 0.13	[0.49 ± 0.02]	[0.22 ± 0.03]	[0.087 ± 0.018]
13	1.5 ± 0.3	0.96 ± 0.13	[0.71 ± 0.09]	[0.27 ± 0.05]
14	0.57 ± 0.16	[0.13 ± 0.02]	[0.068 ± 0.011]	···
15	1.6 ± 0.4	[0.490 ± 0.014]	[0.26 ± 0.04]	···
16	[0.33 ± 0.03]	[0.074 ± 0.006]	[0.030 ± 0.009]	···
17	[0.71 ± 0.08]	[0.072 ± 0.004]	[0.026 ± 0.006]	···
18	[0.176 ± 0.018]	[0.036 ± 0.004]	···	···
19	[0.46 ± 0.06]	[0.0130 ± 0.0009]	···	···
20	···	[0.0031 ± 0.0005]	···	···
21	···	[0.0118 ± 0.0008]	···	···

[a] Values in parentheses (square brackets) denote estimated populations (uncalibrated ion signals); see text. Uncertainties represent one standard deviation.

circles connected by dotted lines in the figures). These levels were not used in the normalizations employed to compare the present results with other experimental or theoretical results (Discussion section), but they were included in the calculation of the vibrational distribution (see below).

Vibrational branching ratios were determined by measuring the population ratio of two rotational levels in adjacent vibrational states. The relation between the population in a given rovibrational level and the total population in that vibrational state is known from the measured rotational distributions (Table I). Therefore, the vibrational branching ratio can be calculated from this measurement (along with the vibrational correction factor from the calibration).[16] In calculating the vibrational branching ratios, two approxima-

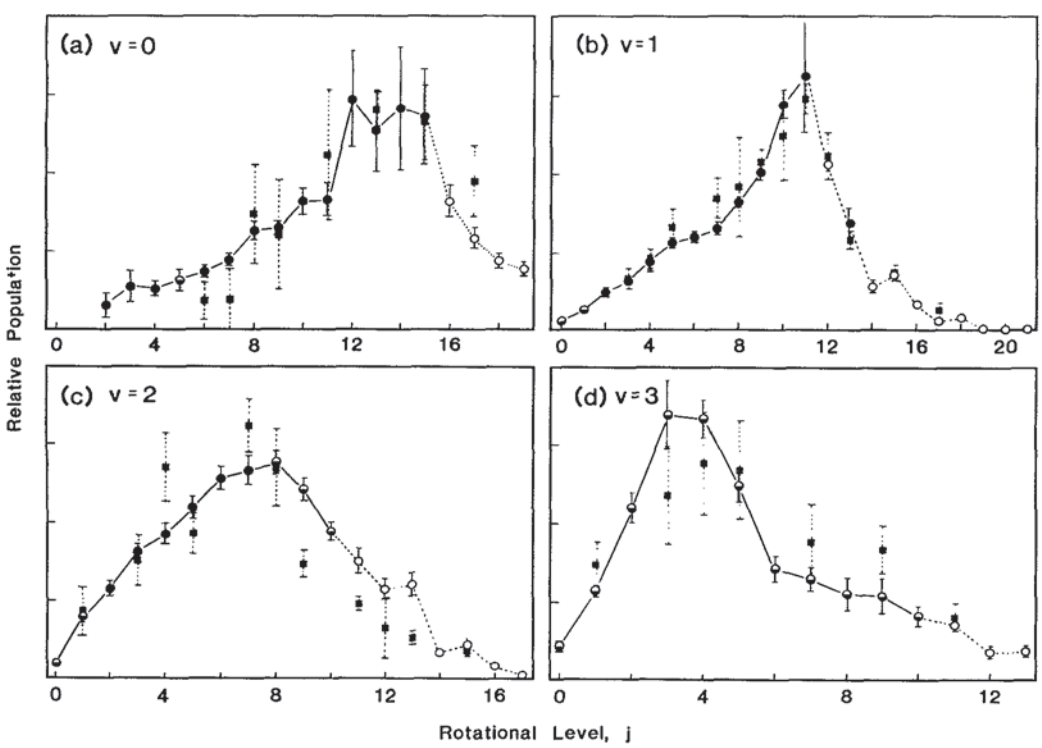

FIG. 2. Rotational population distributions of the $H_2(v, j)$ product of the H + HI reaction for (a) $v=0$, (b) $v=1$, (c) $v=2$, and (d) $v=3$. Circles with solid error bars denote the results of the present experiment; squares with dotted error bars denote the experimental results of AGV. Error bars represent one standard deviation.

tions were made: (1) The populations of all unmeasured levels were taken as zero, which should be an insignificant error because most energetically accessible rotational levels in each vibrational state were observed; and (2) the "uncalibrated ion signals" were included in the total population of each vibrational state, making the calculated total population a lower limit on the actual population [see point (iii) above]; this should again represent only a small error, especially with respect to the relatively large error bars on the vibrational branching ratios. No experimental vibrational correction factor for $v=3$ is available;[16] however, an estimated value based on theoretical calculations of the two-photon transition moments[27] was used to determine the branching ratio into the (minor) $H_2(v=3)$ channel. For $H_2(v=1)$ and $H_2(v=2)$, the experimental correction factors are ~20% less than the theoretical values.[16] Theoretical calculations[27] indicate that REMPI is 1.8 times more sensitive to $H_2(v=3)$ than to $H_2(v=0)$; therefore, we used an $H_2(v=3)$ correction factor of 1.4 ± 0.3. Vibrational branching ratios are given in Table II and the vibrational population distribution is displayed in Fig. 3.

The available energy is sufficient to populate product vibrational states up to $v=7$. We observed $H_2(v=4)$ product from the probe-laser-induced $H+HI$ reaction, but found no enhancement by the photolysis laser, probably because less than 5% of the HI was photolyzed under our experimental conditions. AGV measured populations of 2 rotational levels of $H_2(v=4)$, and found no evidence for the population of higher vibrational states.

IV. DISCUSSION

A. Product internal-state distribution

As shown in Figs. 2 and 3, the H_2 product of the $H+HI$ reaction is formed with a high degree of internal excitation. Of the 3.1 eV of energy available to the reaction products, approximately 23% is partitioned into product rotation, 20% into product vibration, and, therefore, 57% (1.8 eV) into product translation. The measured rotational and vibrational distributions are not well characterized by linear surprisal plots.[1] The H_2 rotational distributions for $v=0$ and $v=1$ cannot be described by temperatures, but those for $v=2$ and $v=3$ are reasonably well fit by temperatures of 7000 and 3000 K, respectively.

The high degree of rotational excitation (Fig. 2) suggests that the HHI PES does not have a strong preference for collinearity at the transition state, which is consistent with semiempirical PESs for this system. According to the surface of Baer and Last,[28] HHI bend angles of less than 90° are accessible at $E_{rel}=1.61$ eV.

TABLE II. $H+HI \rightarrow H_2(v)+I$ vibrational branching ratios.

v	Relative population[a]
0	0.60 ± 0.15
1	1.00
2	0.58 ± 0.23
3[b]	0.24 ± 0.14

[a] Uncertainties represent one standard deviation.
[b] Using estimated vibrational correction factor for $v=3$; see text.

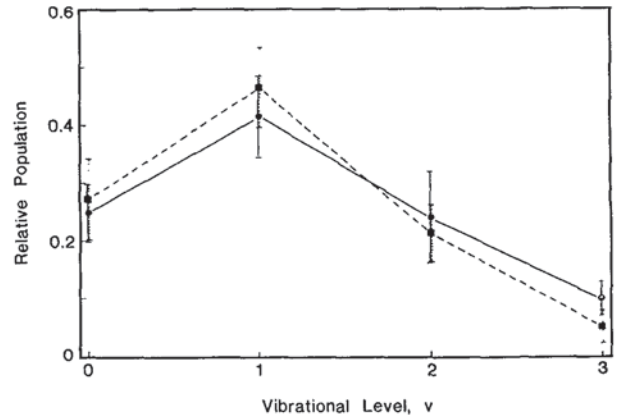

FIG. 3. Vibrational population distribution of the H_2 product of the $H+HI$ reaction. Circles with solid error bars denote the results of the present experiment; squares with dashed error bars denote the experimental results of AGV. Error bars represent one standard deviation.

As discussed in the Introduction, AGV noted that the highest populated rotational level in each vibrational state has an energy approximately equal to the reaction exoergicity plus $E_{rel}/2$ ($j=19$, 17, 14, and 11 in $v=0$, 1, 2, and 3, respectively). Although we observed rotational levels above this energetic "cutoff," their populations are relatively small, consistent with the interpretation of AGV. These high-j levels are rather remarkable. For example, the $H_2(v=1, j=21)$ level has 2.6 eV of rotational energy.[2] We know of no other reaction that produces such rotationally hot H_2. The $H+HI$ reaction has been used as a source of excited H_2 for spectroscopic studies.[29]

The vibrational inversion (Fig. 3) is a reflection of the early barrier characteristic of highly exothermic reactions.[1,3] As discussed in the Introduction, the energy available to product vibrational excitation is limited, however, by the kinematic constraint imposed by the 45° skew angle. In addition, the high energy with respect to the barrier at which these experiments were carried out enables trajectories far from the minimum energy path of the PES to contribute to reaction. In particular, AGV suggested that trajectories that do not effectively couple reagent translation into product vibration are of importance, further limiting the amount of H_2 vibrational excitation.

Sufficient energy is available to produce electronically excited I* by the reaction $H+HI \rightarrow H_2+I^*$. This channel has been found to be minor at thermal energies;[6] ion-imaging measurements indicate, however, that it contributes at higher collision energies.[7] No feature of the present internal-state distribution can be ascribed to this reaction pathway.

B. Comparison with previous experiment

The present experimental results are directly comparable to those of AGV. Because CARS has a lower sensitivity than REMPI, AGV observed approximately half of the levels seen in the present experiment with error bars typically 2–3 times as large. In the present REMPI study, however, all

of the levels populated by the H + HI reaction could not be calibrated with the thermal calibration source (see Results section), a problem that is not applicable to CARS. Where a comparison is possible, the agreement between the two experiments is excellent, as shown in Figs. 2 and 3 for the rotational and vibrational population distributions, respectively.

The quantitative agreement between the present results and those of AGV is significant because of the substantially different experimental methodologies employed. In previous comparisons between REMPI and CARS measurements for the $H+D_2$ reaction, comparable agreement was observed.[20,30] Conversely, for the H + *para*-H_2 reaction, substantial discrepancies exist,[21,31] which has led to speculation that a nonlinear effect may interfere with the interpretation of the CARS spectra.[32,33] For the present study, the excellent agreement between the two experiments gives confidence that the measurements are correct and that they may be used to test theoretical descriptions of the H + HI abstraction reaction.

C. Comparison with theory

Ab initio PES calculations are difficult for the H + HI system because it possesses a large number of electrons and relativistic effects may be important. However, several approximate HHI surfaces have been calculated.[28,34–38] Two groups have performed quasiclassical trajectory (QCT) calculations for the H + HI reaction at the collision energies relevant to the present experiment using the common assumption of a single PES.[36,38] To compare with these calculations, we converted their calculated cross sections into rate constants (73% of the 1.61 eV cross section plus 27% of the 0.67 eV cross section) and normalized each rotational distribution to the sum of the populations in common with the experimental distribution. In this normalization, only the experimental "populations" and "estimated populations" were used, not the "uncalibrated ion signals" (see Results section). Comparisons of the experimental rotational distributions with the QCT calculations of González and Sayós (GS)[36] and of Aker and Valentini (AV)[38] are shown in Figs. 4 and 5, respectively.

The QCT calculations of both GS and AV were performed on London–Eyring–Polanyi–Sato (LEPS)[1] semiempirical surfaces. AV also ran trajectories on a diatomics-in-molecules PES including three-center terms (DIM-3C),[28] but found that the LEPS and DIM-3C results were identical within statistical uncertainty. GS restricted the initial state of the HI reagent to ($v=0, j=4$), the most populated rotational level at room temperature, while AV performed a Boltzmann average over initial HI rotational levels. AV found that the state-specific reaction cross sections were insensitive to the initial HI rotational level, as expected for rotationally sudden collisions.[1]

Figure 4 shows that the H_2 ($v=0$) and H_2 ($v=1$) rotational distributions of GS are several quanta colder and somewhat broader than the corresponding experimental distributions. The experimental and theoretical H_2 ($v=2$) rotational distributions are in close agreement, though again the QCT distribution is slightly too cold. For H_2 ($v=3$), the QCT rotational distribution reproduces the shape of the experimental distribution, but it is too hot by 2–3 quanta. Figure 5 shows that the QCT distributions of AV are generally in much better agreement with experiment than are those of GS, though the H_2 ($v=3$) distribution is slightly too hot rotationally.

The vibrational population distributions of the H_2 product of the H + HI reaction obtained from the present experi-

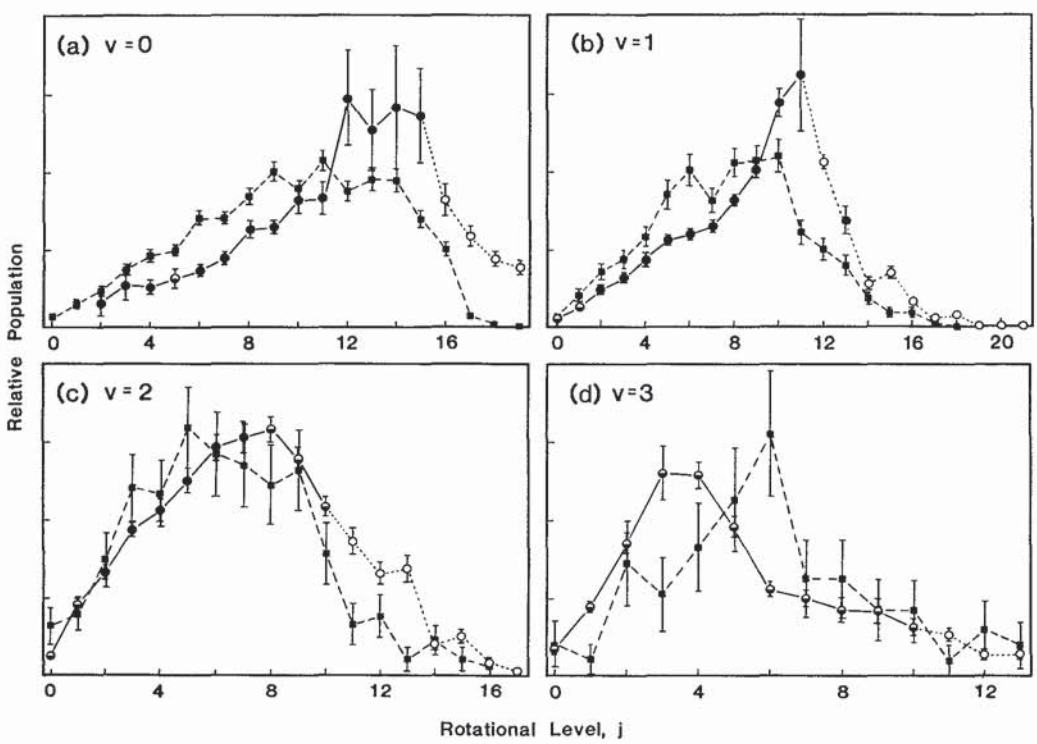

FIG. 4. Comparison of experimental and theoretical rotational population distributions of the H_2 (v, j) product of the H + HI reaction for (a) $v=0$, (b) $v=1$, (c) $v=2$, and (d) $v=3$. Circles denote the results of the present experiment; squares denote the QCT results of GS. Error bars represent one standard deviation.

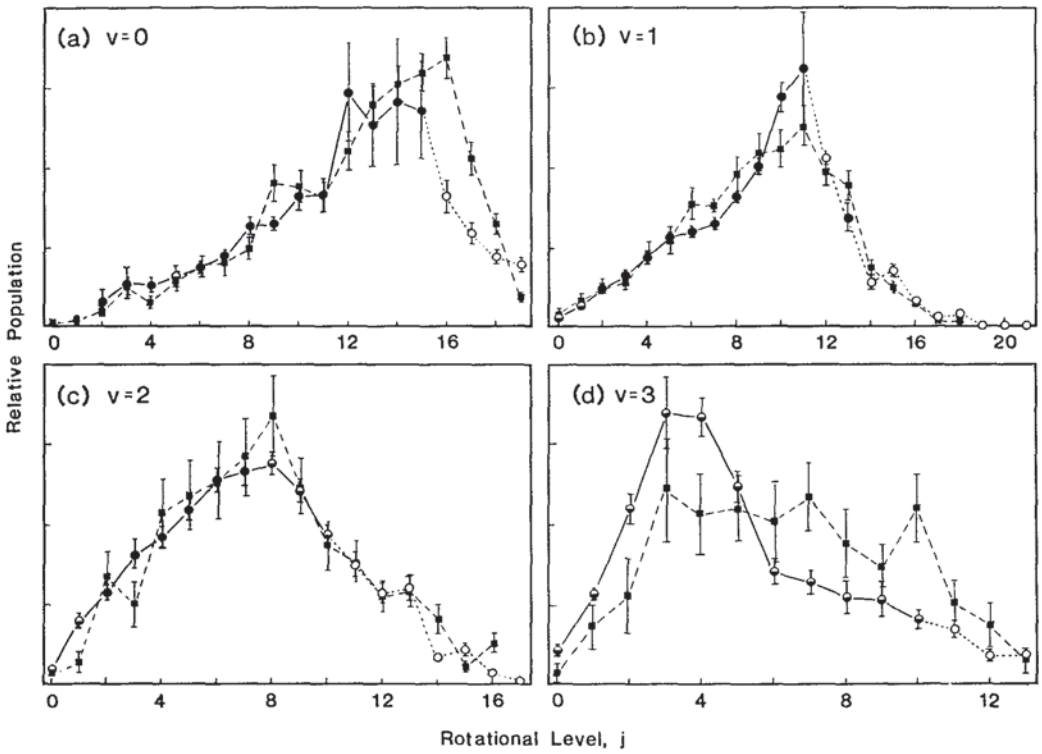

FIG. 5. Comparison of experimental and theoretical rotational population distributions of the $H_2(v, j)$ product of the H + HI reaction for (a) $v = 0$, (b) $v = 1$, (c) $v = 2$, and (d) $v = 3$. Circles denote the results of the present experiment; squares denote the QCT results of AV. Error bars represent one standard deviation.

ment and from the two QCT calculations are compared in Fig. 6. Neither calculation reproduces the vibrational population inversion observed between $v = 0$ and $v = 1$. GS noted that such an inversion is found at low collision energies, but disappears between 0.4 and 0.5 eV. In contrast, AV found a vibrational inversion between $H_2(v = 0)$ and $H_2(v = 1)$ at $E_{rel} = 0.68$ eV, but not at $E_{rel} = 1.60$ eV nor at the 1.60/0.68 eV average applicable to the present experiment.

The inability of the QCT calculations to reproduce the vibrational population inversion between $H_2(v = 0)$ and $H_2(v = 1)$ is the most significant deficiency of these computations and may indicate that further refinement of the HHI PES is necessary for a complete understanding of the dynamics of the H + HI reaction. In addition, quantum-mechanical calculations are required to assess the importance of quantum effects in this system.[39] The role of the $H + HI \rightarrow H_2 + I^*$ channel at superthermal collision energies also requires additional investigation. In conclusion, approximate theoretical treatments of the H + HI abstraction reaction are unable to reproduce all features of the experimentally determined internal-state distribution. This failure stands as a challenge to future theoretical efforts.

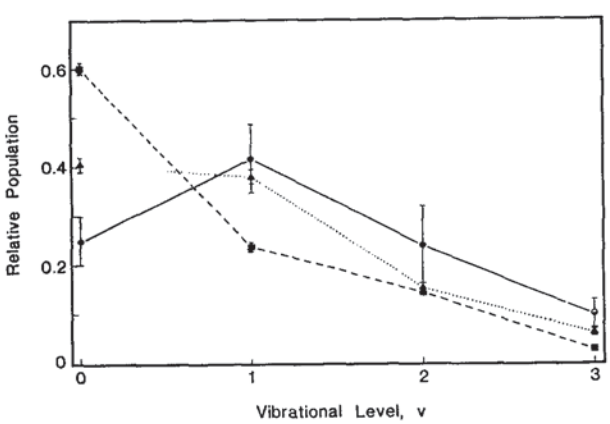

FIG. 6. Comparison of experimental and theoretical vibrational population distributions of the H_2 product of the H + HI reaction. Circles denote the results of the present experiment; squares (triangles) denote the QCT results of GS (AV). Error bars represent one standard deviation.

ACKNOWLEDGMENTS

D. A. V. K. gratefully acknowledges a GAANN graduate fellowship from the U.S. Department of Education. This work was supported by the National Science Foundation under National Science Foundation Grant No. CHE 90-07939.

[1] R. D. Levine and R. B. Bernstein, *Molecular Reaction Dynamics and Chemical Reactivity* (Oxford University, New York, 1987); I. M. W. Smith, *Kinetics and Dynamics of Elementary Gas Reactions* (Butterworths, London, 1980).
[2] K. P. Huber and G. Herzberg, *Molecular Spectra and Molecular Structure IV. Constants of Diatomic Molecules* (Van Nostrand Reinhold, New York, 1979).
[3] J. C. Polanyi, Acc. Chem. Res. **5**, 161 (1972).
[4] H. Umemoto, S. Nakagawa, S. Tsunashima, and S. Sato, Chem. Phys. **124**, 259 (1988).
[5] C. E. Moore, Natl. Bur. Stand. (U.S.) Circ. 467, Vol. 3 (1958).
[6] P. Cadman and J. C. Polanyi, J. Phys. Chem. **72**, 3715 (1968).
[7] M. A. Buntine, D. P. Baldwin, R. N. Zare, and D. W. Chandler, J. Chem. Phys. **94**, 4672 (1991).
[8] T. H. Dunning, Jr., J. Phys. Chem. **88**, 2469 (1984).
[9] A. Persky and A. Kuppermann, J. Chem. Phys. **61**, 5035 (1974).
[10] J. D. McDonald and D. R. Herschbach, J. Chem. Phys. **62**, 4740 (1975).
[11] W. Bauer, L. Y. Rusin, and J. P. Toennies, J. Chem. Phys. **68**, 4490 (1978).

[12] R. E. Continetti, G. N. Robinson, and Y. T. Lee, poster presented at the 1987 Conference on the Dynamics of Molecular Collisions, Oglebay Park, West Virginia (1987).
[13] P. M. Aker, G. J. Germann, and J. J. Valentini, J. Chem. Phys. **90**, 4795 (1989).
[14] R. D. Clear, S. J. Riley, and K. R. Wilson, J. Chem. Phys. **63**, 1340 (1975); R. Schmiedl, H. Dugan, W. Meier, and K. H. Welge, Z. Phys. A **304**, 137 (1982).
[15] P. M. Aker, G. J. Germann, K. D. Tabor, and J. J. Valentini, J. Chem. Phys. **90**, 4809 (1989).
[16] K.-D. Rinnen, D. A. V. Kliner, R. N. Zare, and W. M. Huo, Isr. J. Chem. **29**, 369 (1989); K.-D. Rinnen, M. A. Buntine, D. A. V. Kliner, R. N. Zare, and W. M. Huo, J. Chem. Phys. (in press).
[17] D. A. V. Kliner, K.-D. Rinnen, and R. N. Zare, J. Chem. Phys. **90**, 4625 (1989).
[18] K.-D. Rinnen, D. A. V. Kliner, M. A. Buntine, and R. N. Zare, Chem. Phys. Lett. **169**, 365 (1990).
[19] K.-D. Rinnen, D. A. V. Kliner, R. S. Blake, and R. N. Zare, Rev. Sci. Instrum. **60**, 717 (1989).
[20] K.-D. Rinnen, D. A. V. Kliner, and R. N. Zare., J. Chem. Phys. **91**, 7514 (1989).
[21] D. A. V. Kliner, D. E. Adelman, and R. N. Zare., J. Chem. Phys. **94**, 1069 (1991).
[22] W. J. van der Zande, R. Zhang, and R. N. Zare, in *Spectral Line Shapes*, Vol. 6, edited by L. Frommhold and J. W. Keto (American Institute of Physics, New York, 1990), p. 301; W. J. van der Zande, R. Zhang, R. N. Zare, K. J. McKendrick, and J. J. Valentini, J. Phys. Chem. (in press).
[23] The BBO crystals were supplied by R. S. Feigelson and R. K. Route and grown as part of a research program sponsored in part by the Army Research Office, Contract No. DAAL03-86-K-0129, and in part by the NSF/MRL Program through the Center for Materials Research, Stanford University.
[24] R. S. Blake, Ph.D. thesis, Stanford University, Stanford, CA (1988).
[25] K.-D. Rinnen, D. A. V. Kliner, R. S. Blake, and R. N. Zare, Chem. Phys. Lett. **153**, 371 (1988).
[26] F. J. de Heer, W. Huizenga, and J. Kistemaker, Physica **23**, 181 (1957); we thank B. A. Collings and J. H. Wang (University of Toronto) for calling this reference to our attention.
[27] W. M. Huo, K.-D. Rinnen, and R. N. Zare, J. Chem. Phys. (submitted for publication).
[28] M. Baer and I. Last, in *Potential Energy Surfaces and Dynamics Calculations*, edited by D. G. Truhlar (Plenum, New York, 1981).
[29] G. J. Germann and J. J. Valentini, J. Phys. Chem. **92**, 3792 (1988).
[30] D. P. Gerrity and J. J. Valentini, J. Chem. Phys. **81**, 1298 (1984).
[31] J.-C. Nieh and J. J. Valentini, Phys. Rev. Lett. **60**, 519 (1988); J. Chem. Phys. **92**, 1083 (1990).
[32] J. L. Krause and M. Shapiro, Isr. J. Chem. **29**, 427 (1989); T. Seideman, J. L. Krause, and M. Shapiro, Chem. Phys. Lett. (in press).
[33] J. J. Valentini (private communication).
[34] L. M. Raff, L. Stivers, R. N. Porter, D. L. Thompson, and L. B. Sims, J. Chem. Phys. **52**, 3449 (1970); **58**, 1271 (1973).
[35] C. A. Parr and D. G. Truhlar, J. Phys. Chem. **75**, 1844 (1971), and references therein.
[36] M. González and R. Sayós, Chem. Phys. Lett. **164**, 643 (1989).
[37] C. Parr and A. Kuppermann (unpublished results); parameters given in Ref. 38.
[38] P. M. Aker and J. J. Valentini, Isr. J. Chem. **30**, 157 (1990).
[39] F. M. Chapman, Jr. and E. F. Hayes, J. Chem. Phys. **66**, 2554 (1977).